The DN2 Myeloid-T (DN2mt) Progenitor is a Target Cell for Leukemic Transformation by the TLX1 Oncogene

Lynnsey A Zweier-Renn[1,2], Irene Riz[1], Teresa S Hawley[3] and Robert G Hawley[1,4]*

[1]Department of Anatomy and Regenerative Biology, George Washington University, Washington, DC, USA
[2]Graduate Program in Biochemistry and Molecular Genetics, George Washington University, Washington, DC, USA
[3]Flow Cytometry Core Facility, George Washington University, Washington, DC, USA
[4]Sino-US Joint Laboratory of Translational Medicine, Jining Medical University Affiliated Hospital, Jining Medical University, Jining, Shandong, China

Abstract

Introduction: Inappropriate activation of the TLX1 (T-cell leukemia homeobox 1) gene by chromosomal translocation is a recurrent event in human T-cell Acute Lymphoblastic Leukemia (T-ALL). Ectopic expression of TLX1 in murine bone marrow progenitor cells using a conventional retroviral vector efficiently yields immortalized cell lines and induces T-ALL-like tumors in mice after long latency.

Methods: To eliminate a potential contribution of retroviral insertional mutagenesis to TLX1 immortalizing and transforming function, we incorporated the TLX1 gene into an insulated self-inactivating retroviral vector.

Results: Retrovirally transduced TLX1-expressing murine bone marrow progenitor cells had a growth/survival advantage and readily gave rise to immortalized cell lines. Extensive characterization of 15 newly established cell lines failed to reveal a common retroviral integration site. This comprehensive analysis greatly extends our previous study involving a limited number of cell lines, providing additional support for the view that constitutive TLX1 expression is sufficient to initiate the series of events culminating in hematopoietic progenitor cell immortalization. When TLX1-immortalized cells were co-cultured on OP9-DL1 monolayers under conditions permissive for T-cell differentiation, a latent T-lineage potential was revealed. However, the cells were unable to transit the DN2 myeloid-T (DN2mt)-DN2 T-lineage determined (DN2t) commitment step. The differentiation block coincided with failure to upregulate the zinc finger transcription factor gene Bcl11b, the human ortholog of which was shown to be a direct transcriptional target of TLX1 downregulated in the TLX1+ T-ALL cell line ALL-SIL. Other studies have described the ability of TLX1 to promote bypass of mitotic checkpoint arrest, leading to aneuploidy. We likewise found that diploid TLX1-expressing DN2mt cells treated with the mitotic inhibitor paclitaxel bypassed the mitotic checkpoint and displayed chromosomal instability. This was associated with elevated expression of TLX1 transcriptional targets involved in DNA replication and mitosis, including Ccna2 (cyclin A2), Ccnb1 (cyclin B1), Ccnb2 (cyclin B2) and Top2a (topoisomerase IIα). Notably, enforced expression of BCL11B in ALL-SIL T-ALL cells conferred resistance to the topoisomerase IIα poison etoposide.

Conclusion: Taken together with previous findings, the data reinforce a mechanism of TLX1 oncogenic activity linked to chromosomal instability resulting from dysregulated expression of target genes involved in mitotic processes. We speculate that repression of BCL11B expression may provide part of the explanation for the observation that aneuploid DNA content in TLX1+ leukemic T cells does not necessarily portend an unfavorable prognosis. This TLX1 hematopoietic progenitor cell immortalization/T-cell differentiation assay should help further our understanding of the mechanisms of TLX1-mediated evolution to malignancy and has the potential to be a useful predictor of disease response to novel therapeutic agents in TLX1+ T-ALL.

Introduction

T-cell acute lymphoblastic leukemia (T-ALL) is classified into subtypes based on recurring chromosomal translocations involving transcription factor genes and the gene signature associated with the stage of T-cell developmental arrest [1-3]. The TLX1 homeobox gene (T-cell leukemia homeobox 1, previously known as HOX11) defines a major subtype representing up to 30% of T-ALLs [4,5]. As a result of t(10:14)(q24;q11) and t(7:10)(q35;q24) chromosomal translocations that juxtapose the intact TLX1 gene to T-cell receptor δ and β regulatory sequences, the TLX1 protein is aberrantly expressed at high levels in thymocytes in which it is otherwise absent [6-9]. These observations suggested that deregulation of TLX1 is an initiating event in T-ALL. Murine models of TLX1+ T-ALL have provided support for this hypothesis. However, the long latency of T-cell tumor formation and clonal nature of the resulting malignancies indicated the requirement for additional mutations [10-13]. Multiple lines of investigation have implicated dysregulated expression of TLX1 target genes involved in the mitotic spindle assembly checkpoint that predispose to Chromosomal Instability (CIN) and aneuploidy, as contributing to TLX1-mediated leukemogenesis [12,14-16].

In vitro approaches have also demonstrated the potential of TLX1 to disrupt normal hematopoietic processes and promote the immortalization of murine progenitor cells derived from various

hematopoietic sources, including bone marrow, fetal liver, yolk sac and embryonic stem cells [11,17-21] (reviewed in [22]). Several studies have provided evidence that TLX1 induces progenitor immortalization by blocking differentiation while concurrently increasing replicative capacity [23-27]. We previously reported that transduction of primary murine bone marrow progenitors with TLX1 retroviral vectors readily yields immortalized cell lines [11,17,21]. These TLX1-immortalized cell lines display a strict dependence on interleukin 3 (IL-3; multi-colony stimulating factor) for their survival and proliferation in culture, retain a diploid karyotype and are not leukemogenic when injected into sublethally irradiated syngeneic mice [17,28]. The cell lines express surface antigens that are present on precursors of multiple hematopoietic lineages but their combined morphological and phenotypic properties are most compatible with immature cells belonging to the myeloid lineage [11,17]. We suggested that they might represent a bipotential monocytic-granulocytic precursor since they can be stimulated to partially differentiate along the monocyte/macrophage and granulocyte lineages (into CD11b/Mac-1+ Ly-6G/Gr-1+ cells) upon treatment with phorbol myristate acetate [21].

Within the murine hematopoietic system, the zinc finger transcription factor Bcl11b has been demonstrated to control a restriction point during T-cell differentiation [29-32] (reviewed in [33]). Bcl11b expression downregulates hematopoietic stem and progenitor cell genes and is necessary for T-lineage commitment [31]. Retroviral expression of TLX1 in fetal liver precursors assayed in fetal thymic organ cultures [34] and in transgenic mice under the control of the Lck proximal promoter [10,12] resulted in differentiation arrest at the double-negative 2 (DN2) stage of thymocyte development. A similar arrest of progenitors was observed in thymocytes of mice deficient in Bcl11b [32]. Notably, deletion of Bcl11b still allowed DN2 cells to retain full capability to generate CD11b/Mac-1+ Ly-6G/Gr-1+ myeloid cells if transferred to myeloid-supportive culture conditions [31]. Additionally, De Keersmaecker et al. reported that BCL11B is a direct transcriptional target of TLX1 in human T-ALL using the cell line ALL-SIL, where BCL11B was upregulated after TLX1 knockdown [12].

In view of the above findings, and parallels between the TLX1-immortalized cells and previously described IL-3-dependent T lymphocyte progenitor cell lines in their expression of low levels of the thymocyte differentiation antigen Thy-1/CD90 [11,17,35], we sought to investigate whether the TLX1-derived bone marrow cell lines represent the equivalent of immortalized DN2 thymocyte progenitors.

Materials and Methods

Cell lines and culture conditions

The murine IL-3-dependent bone marrow DN2mt progenitor [17,21,28], PGMD1 [36] and M-NSF-60 (ATCC No. CRL-1838; American Type Culture Collection, Manassas, VA) cell lines were routinely maintained in Iscove's Modified Dulbecco's Medium (IMDM; Mediatech Inc., Herndon, VA) containing 4 mM L-glutamine, 50 IU/ml penicillin, 50 μg/ml streptomycin, 10% heat-inactivated fetal bovine serum (FBS, Cambrex BioScience Walkersville, Inc., Walkersville, MD), 10% conditioned medium from X630-rIL3 cells (a source of recombinant IL-3) plus/minus 0.75 mg/ml geneticin (Invitrogen Corp., Carlsbad, CA) as applicable. Murine TLX1+ CD4+CD8+ double-positive THY137 T-ALL-like cells [11], WEHI-3 cells (ATCC No. TIB-68) and M1 cells (ATCC No.TIB-192) cells, and human TLX1+ ALL-SIL cells [6] were maintained in IMDM containing 4 mM L-glutamine, 50 IU/ml penicillin, 50 μg/ml streptomycin and 10% heat-inactivated FBS.

Phoenix-Eco packaging cells (ATCC no. SD 3444), 293T cells (ATCC no. CRL-11268) and NIH3T3 fibroblasts (ATCC No. CRL-1658) were cultured in Dulbecco's Modified Eagle Medium (DMEM; Mediatech, Inc.) supplemented with 4.5 g/l glucose, 4 mM L-glutamine, 50 IU/ml penicillin, 50 μg/ml streptomycin and 10% heat-inactivated FBS. OP9-Delta-like-1 cells (OP9-DL1; gift from Juan Carlos Zúñiga-Pflücker, University of Toronto, Toronto, ON) were maintained in Minimum Essential Medium Alpha Medium (αMEM, Invitrogen Corp.) supplemented with 20% heat-inactivated FBS, 1% non-essential amino acids (NEAA; Invitrogen Corp.) and 50 IU/ml penicillin, 50 μg/ml streptomycin. All cells were maintained at 37°C in a humidified incubator containing 5% CO_2.

Construction of retroviral expression vectors

The plasmids used for expression of TLX1 were constructed as follows. The EcoRI f-HOX11/TLX1 fragment from pGEX-4T-1-fHOX11 [27] was blunt-end cloned into BamHI-digested MSCV-IRES-GFP to form MSCV-flag-TLX1-IR-GFP. The flag-TLX1 gene was removed by NcoI digestion of the MSCV-flag-TLX1-IR-GFP plasmid and subcloned into NcoI-digested RMSinOFB, an insulated self-inactivating (SIN) retroviral vector [37], to produce the RMSin-flag-TLX1-IR-GFP-OFB plasmid. Plasmids were confirmed by restriction digestion with multiple enzymes and agarose gel electrophoresis. The plasmids used for expression of EML1-ABL1, NOTCH1 and BCL11B were: MSCVpuro-EML1-ABL1 (a gift from Jan Cools, Vlaams Instituut voor Biotechnologie, Leuven, Belgium) [38], Mig ICN1-IRES-GFP (a gift from Warren Pear, University of Pennsylvania, Philadelphia, PA) [39] and MSCV-BCL11B (a gift from Dorina Avram, Albany Medical College, Albany, NY) [40]. Controls were: MSCVpuro [41] and MSCV-IRES-GFP [37].

Production of retroviral supernatants

Ecotropic or amphotropic retroviral vector particles were generated by transient transfection using calcium phosphate coprecipitation as described previously [37]. Briefly, plasmid DNA was prepared using the QIAfilter Plasmid Maxi Kit (Qiagen, Valencia, CA). To produce ecotropic retroviral particles, Phoenix-Eco cells were transfected with retroviral vector plasmids. To produce amphotropic retroviral particles, 293T cells were transfected with the retroviral vector plasmid and the amphotropic packaging plasmid. Viral supernatants were collected after 24 and 48 hours and filtered through a 0.45-um-pore-size filter (Nalgene Nunc International, Rochester, NY) before aliquoting and freezing at -80°C for future transductions. When necessary, ecotropic vector-conditioned medium was concentrated by overnight centrifugation at 9,000 g. Vector titers were measured on NIH3T3 cells by flow cytometric analysis of GFP fluorescence using a FACSCalibur instrument (BD Biosciences, San Jose, CA) as described previously [37].

TLX1 hematopoietic progenitor cell immortalization assay

The bone marrow progenitor replating assay was performed as described previously [37,42] with modifications as follows. Bone marrow cells were harvested from BALB/c mice at 6 to 8 weeks of age 4 days after intraperitoneal injection of 5-FU (150 mg/kg body weight) and cultured in IMDM supplemented with 10% heat-inactivated FBS and 10% X630-rIL3 CM, Sp2/rIL-6 CM (interleukin-6), and CHO-KLS CM (stem cell factor) [43]. Bone marrow processing, transduction, and GFP expression analysis were carried out as described previously [37]. All animal procedures were carried out in accordance with The George Washington University Institutional Animal Care and Use Committee guidelines. After 48 hours of prestimulation, bone marrow cells were

transferred to plates coated with full-length human fibronectin (BD Biosciences) and transduced with RMSin-flag-TLX1-IR-GFP-OFB for three consecutive days (4 hours each day) by incubation with vector-conditioned medium and 8 µg/ml polybrene. Transduced cells were cultured in IMDM supplemented with 10% heat-inactivated FBS and 10% X630-rIL3 CM during which time the cells were passaged every 2 days. After bulk culture for 2 weeks, 10 or 100 cells were plated into each well of a 96-well plate and cultured. Four weeks post plating, the plates were examined, and the replating frequency was determined on the basis of the number of wells that contained proliferating cell populations. Transduced bone marrow cells were cultured until immortalized cell lines were established.

Retroviral insertional mutagenesis analysis

Linker-Mediated nested Polymerase Chain Reaction (LM-PCR) was performed as previously described [28] with modifications that allowed the identification of genomic regions adjacent to RMSin-f-TLX1-OFB vector sequences. Briefly, genomic DNA was isolated from cell lines using the GenElute Mammalian Genomic DNA Kit (Sigma) and digested with Tsp509I (New England Biolabs). The restriction enzyme was removed by phenol chloroform extraction and the DNA was ligated to the linker specific for the Tsp509I overhang (5'-GACCCGGGAGATCT-GAATTCAGTGGCACAGCAGTTAGG-3' and 5'-AATTCCTAACT-GCTGTGCCACTGAATTCAGATC-3').Primary PCR was performed using primers complementary to the linker (5'-GACCCGGGAGA-TCTGAATTC-3') and the RMSin-f-TLX1-OFB vector sequence (5'-ACTGGCGCCTGCAGGCATGC -3') under the following conditions: 30 cycles at 95°C for 15 sec, 60°C for 30 sec, and 72°C for 1 min. Secondary PCR was performed using nested primers (5'-AGTGGCACAG-CAGTTAGG-3' and SIN, 5'- GCAGGCCTGGGACTAGTTG -3') after a 1:50 dilution of the primary PCR product under the same conditions as above. The RMSinOFB primers used in this study were previously used to detect the SIN LTR sequence [37]. Nested PCR products were separated by gel electrophoresis on 1% agarose gels in TAE buffer and bands excised and purified using the Qiagen MinElute Gel Extraction Kit (Qiagen). All PCR amplifications were performed using Platinum Taq (Invitrogen). PCR products were cloned into the pCR4-TOPO vector and transformed into TOP10 cells (Invitrogen). DNA was isolated from ampicillin resistant colonies using the QIAprep Spin Miniprep Kit (Qiagen) and sequenced using an M13 reverse primer.

Proviral junctions from LM-PCR clones were examined for the presence of the linker cassette primer, LTR primer, and 5' LTR sequences. The integrations were considered valid if the end of the 5' LTR was less than two base pairs from the matching genomic sequence within the integration and if there was at least 90% homology to the mouse genome. Sequences were analyzed with CLC Free Workbench (CLCBio USA, Cambridge, MA). Integration sites were identified by matching sequences to the mouse genomic build of July 2007 (National Center for Biotechnology Information Build 37) using the UCSC genome browser (http://genome.ucsc.edu/). Vector orientation and location of the vector with respect to the nearest gene were determined. Hits in the Mouse Retrovirus Tagged Cancer Gene Database (RTCGD; http://rtcgd.abcc.ncifcrf.gov/) [44] and the Insertional Dominance Database (IDDb; http://www99.mh-hannover.de/kliniken/zellth/method.html) associated with hematopoietic clonal expansion [45] were identified for the nearest gene and genes within 100 kb of the integration sites.

Deletion analysis of Cdkn2a (p16^{Ink4a}/p19^{Arf}) and Cdkn2b (p15^{Ink4b}) tumor suppressor genes

Genomic DNA (200 ng) from TLX1-expressing cell lines and pri-

mary bone marrow progenitor cells was isolated using genomic DNA was extracted using the GenElute Mammalian Genomic DNA Kit (Sigma). p15 (Ink4b, exon 2) and p16 (Ink4a, exon 2) were amplified from genomic DNA using primers previously published by Haviernik et al. [46]; p15 forward 5'-GTCATGATGATGGGCAGCG-3', reverse 5'-CAATCTCCAGTGGCAGCGTG-3'; p16 forward 5'-GATGATGAT-GGGCAACGTTC-3', reverse 5'-GTCCTCGCAGTTCGAATCTGC-3'. PCR was performed using Taq DNA polymerase (Roche Diagnostics) under the following conditions: 30 cycles at 94°C for 30 sec, 65°C for 1 min, and 72°C for 1 min. PCR products were separated on a 1% agarose gel.

Transcriptional analysis of Cdkn2a (p16^{Ink4a}/p19^{Arf}), Cdkn2b (p15^{Ink4b}) and p53 tumor suppressor genes

Total RNA was extracted using Trizol reagent. RNA (1 µg) was reverse-transcribed into cDNA using the QuantiTect Reverse Transcription Kit (Qiagen). PCR was performed using Taq DNA polymerase (Roche Diagnostics) under the following conditions: 35 cycles at 94°C for 30 sec, 65°C for 1 min and 72°C for 1 min. RT-PCR products were separated on a 1.5% agarose gel. Primers were designed using Primer 3 software (http://primer3.sourceforge.net/) to span across introns such that PCR amplification of genomic DNA sequences results in a product that is larger in size than the product amplified from the corresponding cDNA templates. In addition, the primers were designed so that the size of the RT-PCR product was similar in size to the housekeeping gene glyceraldehyde-3-phosphate dehydrogenase (Gapdh) RT-PCR product to ensure similar amplification efficiency:

Gapdh (NM_008084.2) forward 5'-ATCCCAGAGCTGAACG-3', reverse 5'-GAAGTCGCAGGAGACA-3'; Gata1 (NM_008089.1) forward 5'- AGGCACCCAATGCACTAACT-3', reverse 5'- TCCTC-GTCTGGATTCCATCT-3'; Eif4a2 (NM_013506.2) forward 5'-ACAATGCCAACTGATGTGCT-3', reverse 5'- ACCTTGCGCCTT-GTATTGAG-3'; Rab27b (NM_030554.3) forward 5'- CAACTGCAG-GCAAATGCTTA-3', reverse 5'- GTGTCCGGAACCTGTGTCTT-3'; Ubash3b (NM_176860.5) forward 5'- ACCTCACATTCCAGT-CAGCA-3', reverse 5'- TGACAGGTACACGCTTCGAG-3'; Spns2 (NM_153060.2) forward 5'- AGTTCCTGAGCCTGGGCTAT-3', reverse 5'- GACTTTCACGGATGCAGGAG-3'; Eno3 (NM_007933.2) forward 5'- TGGACCTCATTCCTCTCTGG-3', reverse 5'- CAT-CACTCCCCAGCCATTAG-3'; Il4ra (NM_001008700.3) forward 5'- CTGATACAGCGCCTTCCACT-3', reverse 5'- AATGATGAT-GGCCACCAAGG-3'; Ndufb10 (NM_026684.2) forward 5'- AG-CAGAGGGAGGGAGAGAAC-3', reverse 5'- GCCTTCCTTTCTTC-CAGCAT-3'; Fut7 (NM_013524.2) forward 5'- GACAATTC-CAGAAGGCTCCA-3', reverse 5'- GAAAGGCCAGTGCCAGATAA-3'; p53 (NM_011640.3) forward 5'- GCCCCTGTCATCTTTTGT-3', reverse 5'- CTTCGCCAGCTGGCAGAATAGC-3' with annealing temperature of 60°C; p15 (NM_007670.4) forward 5'- GTTGGGCG-GCAGCAGTGAC-3', reverse 5'- CAATCTCCAGTGGCAGCGTG-3' with annealing temperature of 70°C; p16 (NM_001040654.1) forward 5'- GTACCCCGATTCAGGTGATG-3' with annealing temperature of 55°C, reverse 5'- TCGCACGATGTCTTGATGTC-3'; p19 (NM_009877.2) forward 5'- GTCGCAGGTTCTTGGTCACTGT-GA-3', reverse 5'- GTCCTCGCAGTTCGAATCTGC-3' with annealing temperature of 70°C. All primers were validated using genomic DNA.

p53 gene mutation analysis

Total RNA was extracted from cell lines using Trizol reagent (Invitrogen). RNA (1 µg) was reverse-transcribed into cDNA using the High-Capacity cDNA Reverse Transcription kit from Applied Biosystems. p53 was amplified from the cDNA using primers previously published

by Yin et al. [47]: (p53 FL forward 5'- CTAGATCTACCATGACTGC-CATGGAGGAGTCAC-3', reverse 5'- AACCTCGAGGTCTGAGT-CAGGCCCCACTTT-3'). PCR products were gel purified using the Qiagen MinElute Gel Extraction Kit (Qiagen) and sequenced using the PCR primers and the following sequencing primers. Sequencing primers (p53 seq forward 5'- TGGAAGACTCCAGTGGGAAC-3', reverse 5' CTCCGTCATGTGCTGTGACT-3') were designed using Primer 3 software (http://primer3.sourceforge.net/). Sequences were analyzed with CLC Free Workbench (CLCBio). Sequencing results were compared to the wild-type p53 sequence obtained from NCBI (NM_011640.3).

Retroviral transduction of cell lines

TLX1[+] murine (DN2mt) or human (ALL-SIL) cells were transduced with the following retroviral vectors: MSCVpuro-EML1-ABL1, MSCVpuro; Mig ICN1-IRES-GFP, MSCV-BCL11B, and MSCV-GFP. Briefly, cells were spinoculated with viral supernatant in the presence of 8 µg/mL polybrene (Sigma) at 2000 rpm at 16°C for 2 hours prior to incubation with the virus for 4 hours at 37°C. Cells transduced with the puromycin resistance-encoding vectors were selected with 2 µg/ml puromycin (Sigma) for 24 hours, allowed to recover, and selected for an additional 24 hours. Cells transduced with GFP vectors were sorted using a FACSAria instrument (BD Biosciences).

T cell differentiation co-cultures

Primary murine bone marrow progenitor cells [37], TLX1/EML1-ABL1 and TLX1/EML1-ABL1-ICN1 cell lines were seeded on confluent monolayers of OP9-DL1 in 50% αMEM and 50% IMDM in the presence of recombinant murine FMS-like tyrosine kinase 3 ligand (Flt3L; 5 ng/ml) and interleukin-7 (IL-7; 1 ng/ml) (Peprotech, Rocky Hill, NJ). Cells were passaged onto fresh monolayers every 4 to 5 days [48-50]. Analysis of cell surface markers was performed as described previously [34]. Fc receptors were blocked with anti-mouse CD16/CD32 (eBioscience). Cells were washed and stained for surface expression of differentiation antigens in Phosphate Buffered Saline (PBS) plus 2% FBS. Cells were immunophenotyped with the following antibodies: CD25-PerCP-Cy5.5 (eBioscience), CD4-APC (Caltag Laboratories, Burlingame, CA), CD44-APC, CD8-PE; CD11b (Mac-1)-PE, (all from BD Biosciences Pharmingen). T cell differentiation flow cytometry data were acquired on a BD FACSAria instrument and analysis was performed using FACSDiva software (BD Biosciences).

Mitotic checkpoint and cell viability analysis

Flow cytometry was performed to assess mitotic checkpoint integrity by cell cycle analysis in cells treated with vehicle control and 0.1 µM paclitaxel (Sigma) for 24 hours or 0.01 µM paclitaxel for 48 hours [51]. Cells were washed in PBS and fixed with 70% ethanol. Cells were rehydrated and washed with PBS prior to staining with PI/RNase A solution (BD Biosciences Pharmingen). Cell cycle flow cytometry data were acquired using CellQuest software on a FACScan instrument (Becton Dickinson). Analysis was performed using ModFit LT software (Verity Software House, Inc., Topsham, ME).

Cells were treated with different concentrations of etoposide (Sigma) as described previously [52] and cell viability was measured using the alamarBlue reagent [53,54].

Quantitative real time RT-PCR (qRT-PCR)

Total RNA was extracted from cell lines using Trizol reagent (Invitrogen). RNA (1 µg) was reverse-transcribed into cDNA using the QuantiTect Reverse Transcription Kit (Qiagen). For knockdown and coculture experiments, RNA for qRT-PCR was extracted using the Power

SYBR Green Cells to CT Kit (Ambion, Austin, TX). The resulting cDNA was diluted and used as a template for quantitative PCR (qPCR) using Power SYBR Green PCR Master Mix (Applied Biosystems). Primers were designed using Primer 3 software (http://primer3.sourceforge.net/) and tested for specificity by in silico PCR (http://genome.ucsc.edu/cgi-bin/hgPcr?command=start). Amplicon specificity was verified by first-derivative melting curve analysis using software provided by PerkinElmer and Applied Biosystems. Quantitation and normalization of relative gene expression were performed using the comparative threshold cycle method (ddCt).

The expression of the housekeeping genes Gapdh (NM_008084.2; forward 5'-GTGAAGGTCGGTGTGAACG-3', reverse 5'- TTGCC-GTGAGTGGAGTCATA-3') and Actb (beta actin; NM_007393.3; forward 5'- CTGTATTCCCCTCCATCGTG-3', reverse 5'- CAT-GTCGTCCCAGTTGGTAA-3') were used for normalization: TLX1 (NM_005521.3) forward 5'- CATCGACCAGATCCTCAACA-3', reverse 5'- CAGCCAAGGCCGTATTCTC-3'. cDNA was amplified using primers previously published by Ikawa et al. [32], Bcl11b forward 5'- ATGTTCTCTCAGGCTTCTCC-3', reverse 5'- TGGGA-CACAGTCAAGTTACC-3'; Lmo2 forward 5'- CACCTGGAGT-GTTTCAAATG-3', reverse 5'- TTGGTCCACTCGTAGATGTC-3'; CD3e forward 5'- ATAGGAGAGACATCGCCTTC-3', reverse 5'-CAGGAGAGCAAGGTTCTAGG-3'. Real-time PCR analysis was performed on an ABI Prism 7900 Sequence Detection System (Applied Biosystems). Each sample was analyzed in triplicate.

Gene expression profiling

RNA samples were analyzed using an Affymetrix GeneChip (MG-U74Av2 microarray) as described previously [24,27,53]. In brief, total RNA was extracted using Trizol reagent (Invitrogen) and the RNeasy Mini Kit (Qiagen). RNA was reverse transcribed into cDNA using an HPLC-purified T7-(dT)24 primer (Genset Oligos/Proligo LLC, Boulder, CO). Biotin-labeled complementary RNA (cRNA) synthesis, hybridization, washing, staining and scanning were performed following the manufacturer's protocols (Affymetrix Inc., Santa Clara, CA). Target cRNA from two biological replicates of each cell line was hybridized to two Affymetrix MG-U74Av2 GeneChip oligonucleotide arrays. Data analysis was performed with GeneSpring software (Silicon Genetics, Redwood City, CA).

Results

No common "immortalizing" genes were identified by mapping of insulated retroviral vector integration sites in TLX1-immortalized progenitor cells

In an effort to rule out artifacts due to retroviral insertional mutagenesis, we previously performed a limited survey of 8 TLX1-immortalized cell lines where we failed to identify a common retroviral integration site. Moreover, no insertions into the Evi1 or Prdm16 immortalizing genes [42,55] were observed [28].

Our laboratory developed a safety-modified retroviral vector, RMSinOFB, which incorporates a novel enhancer-blocking element (termed FB) derived from chromatin insulators [37]. As a consequence of reverse transcription, the FB element flanks the retroviral vector backbone upon integration, virtually eliminating hematopoietic immortalizing potential due to insertional mutagenesis. Using the insulated RMSinOFB retroviral vector backbone to express TLX1, we generated an additional 15 cell lines by immortalization of bone marrow progenitor cells. Extensive characterization of these newly established

cell lines again failed to reveal a common retroviral integration site or involvement of the Evi1 or Prdm16 genes (Tables S1-S3). Taken together with our earlier data demonstrating a structure-function correlation between particular domains of TLX1 and its immortalizing potential [21], we conclude that ectopic TLX1 expression is sufficient to initiate the series of events leading to hematopoietic progenitor cell immortalization.
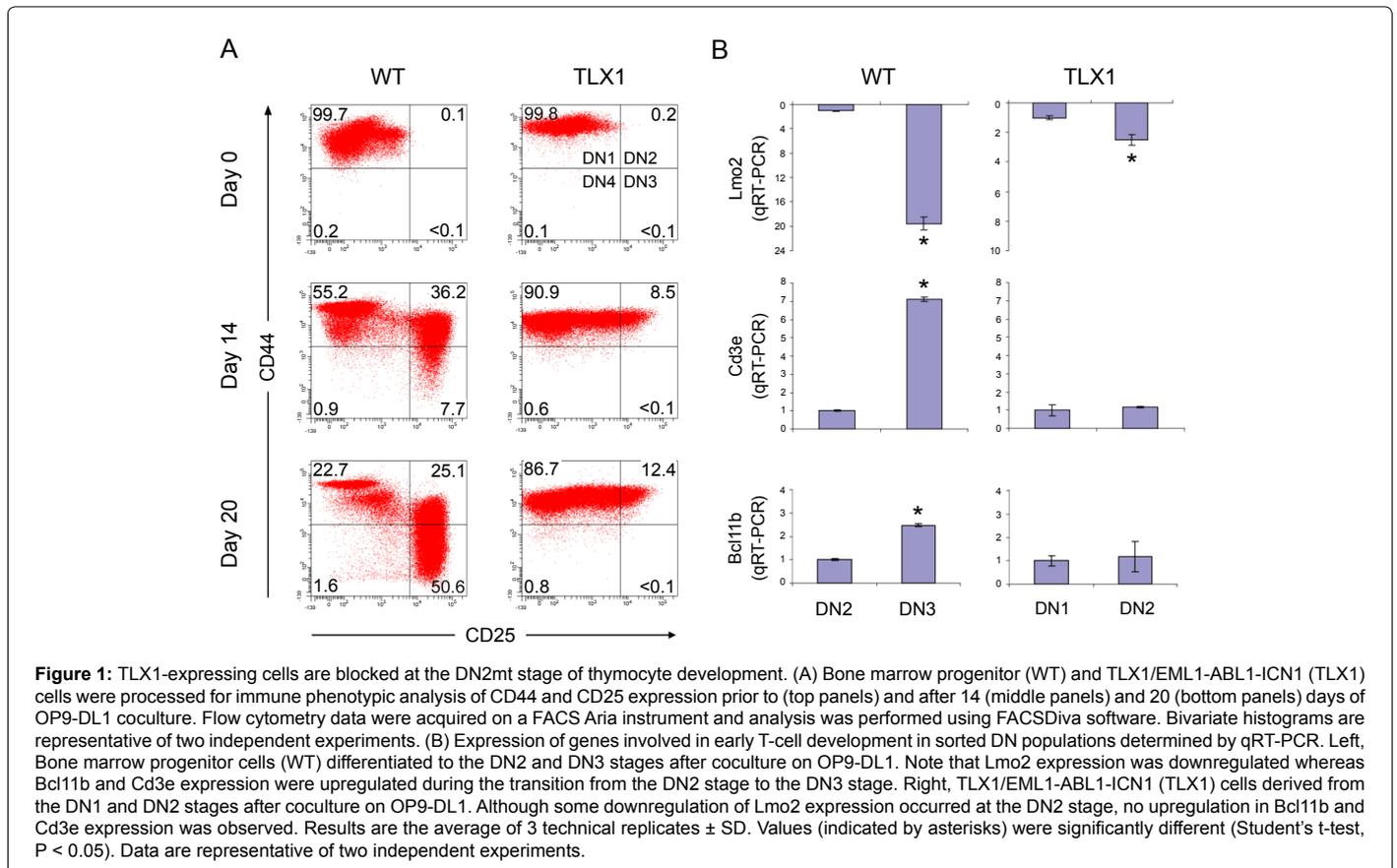
Tumor suppressor genes are intact in TLX1-immortalized hematopoietic progenitor cells

The CDKN2A (previously MTS1) and CDKN2B (previously MTS2) tumor suppressor genes, which encode p16^{INK4a}/p14^{ARF} (p19^{Arf} in the mouse) and p15^{INK4b}, respectively, are frequently inactivated in hematologic malignancies [56]. Both p16^{INK4a} and p15^{INK4b} specifically inhibit cyclin D-CDK4/6 complexes and block cell division during the G_1/S phase of the cell cycle. Furthermore, p14^{ARF}/p19^{Arf} has been shown to positively regulate the p53 tumor suppressor pathway, leading to G_1 cell cycle arrest and/or apoptosis. Studies examining the role of tumor suppressor genes in murine models of immortalization and leukemogenesis have demonstrated frequent deletions in Cdkn2a, Cdkn2b and p53 [46,57-60]. We found no evidence of deletion or complete transcriptional silencing of any of these genes in the TLX1-immortalized cell lines examined (Figures S1 and S2). Moreover, no mutations were found in the p53 genes of four cell lines analyzed. Also, following DNA damage, increased expression of Cdkn1a (a transcriptional target of p53 encoding the CDK inhibitor p21$^{Cip1/Waf}$) was observed coincident with an increase in p53 protein levels (Figure S3), indicating that the p53 pathway was functionally active but actively suppressed in the cells. Survival of the TLX1-immortalized cell lines is clearly dependent on IL-3 [17] and other work has demonstrated that IL-3 signaling promotes hematopoietic cell survival in part by controlling the baseline level and transcriptional activity of p53 [61]. However, given that p53 is a direct TLX1 binding target [12], TLX1 may also play a role in downmodulating p53 levels in these cell lines.

Cell lines established by TLX1-induced immortalization have the potential to differentiate toward the T-cell lineage

EML1-ABL1 and NUP214-ABL1 are fusion genes that arise during the multistep process of TLX1-induced T-ALL development which encode constitutively activated tyrosine kinases. Their acquisition is believed to provide a growth advantage to the leukemic cells [38,62]. It was previously demonstrated that retroviral expression of EML1-ABL1 converted IL-3-dependent Ba/F3 pro-B cells to IL-3-independent growth [38]. In addition, EML1-ABL1 expression in primary bone marrow progenitors induces both T-lymphoid and myeloid leukemias in mice [63]. Therefore, to circumvent the requirement for exogenous IL-3, which is inhibitory to T-cell differentiation [35], we converted the immortalized TLX1-expressing bone marrow progenitor cells to IL-3 independence in an attempt to permit them to differentiate toward the T-cell lineage. IL-3-independent cells were established by ectopic expression of EML1-ABL1 using the MSCVpuro-EML1-ABL1 retroviral vector [38]. Cells were selected for EML1-ABL1 expression using puromycin and IL-3 was removed from the culture medium. Since TLX1+ T-ALLs frequently contain activating NOTCH1 mutations [64], TLX1/EML1-ABL1 cells were also transduced with the Mig-ICN1 retroviral vector which expresses a constitutively activated intracellular form of

Figure 1: TLX1-expressing cells are blocked at the DN2mt stage of thymocyte development. (A) Bone marrow progenitor (WT) and TLX1/EML1-ABL1-ICN1 (TLX1) cells were processed for immune phenotypic analysis of CD44 and CD25 expression prior to (top panels) and after 14 (middle panels) and 20 (bottom panels) days of OP9-DL1 coculture. Flow cytometry data were acquired on a FACS Aria instrument and analysis was performed using FACSDiva software. Bivariate histograms are representative of two independent experiments. (B) Expression of genes involved in early T-cell development in sorted DN populations determined by qRT-PCR. Left, Bone marrow progenitor cells (WT) differentiated to the DN2 and DN3 stages after coculture on OP9-DL1. Note that Lmo2 expression was downregulated whereas Bcl11b and Cd3e expression were upregulated during the transition from the DN2 stage to the DN3 stage. Right, TLX1/EML1-ABL1-ICN1 (TLX1) cells derived from the DN1 and DN2 stages after coculture on OP9-DL1. Although some downregulation of Lmo2 expression occurred at the DN2 stage, no upregulation in Bcl11b and Cd3e expression was observed. Results are the average of 3 technical replicates ± SD. Values (indicated by asterisks) were significantly different (Student's t-test, $P < 0.05$). Data are representative of two independent experiments.
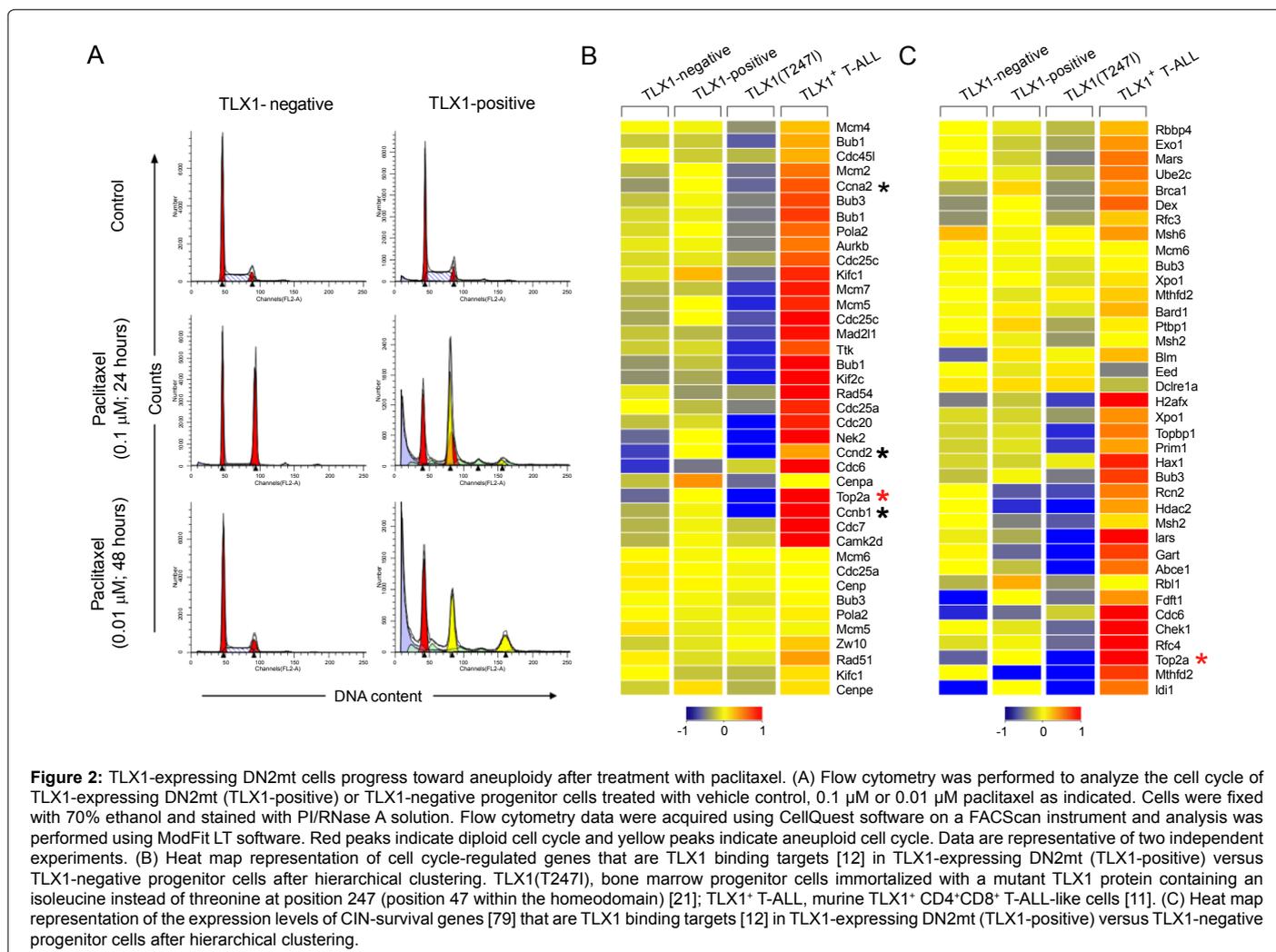
Notch1 [39]. To promote T-cell differentiation, we cultured the TLX1/EML1-ABL1 and TLX1/EML1-ABL1-ICN1 cells on OP9-DL1 stromal cells in medium supplemented with Flt3L and IL-7 [65]. OP9-DL1 coculture provides activation of endogenous Notch [48]. Flt3L provides proliferation signals and IL-7 provides signals for survival, proliferation and differentiation of T-cell progenitors in a dose-dependent fashion [49]. Primary murine bone marrow progenitor cells were used as a positive control for T-cell differentiation potential [49,50].

Early T-cell development in mice proceeds through a DN stage that is subdivided into four populations based on cell surface expression of the hyaluronan receptor (CD44) and the IL-2 receptor α chain (CD25): DN1 (CD44+, CD25-); DN2 (CD44+, CD25+); DN3 (CD44-, CD25+); and DN4 (CD44-, CD25-). Prior to co-culture, bone marrow progenitors, TLX1/EML1-ABL1 and TLX1/EML1-ABL1-ICN1 cells were positive for CD44 and negative for CD25 (Figure 1). In the representative experiment presented in Figure 1, after 14 days in culture, a fraction of the primary bone marrow progenitor cells had differentiated to the DN2 (~36%) and DN3 (~8%) stages of T-cell development. By 20 days, the bone marrow progenitor cell population had further differentiated such that the majority of the cells were at the DN2 (~25%) and DN3 (~51%) stages. By comparison, after 14 days of culture, a fraction of the TLX1/EML1-ABL1 and TLX1/EML1-ABL1-ICN1 cultures had differentiated to the DN2 stage (~8%) (Figure 1; and data not shown).

By day 20, the percentage of cells in the DN2 stage had increased to ~12%. However, the cells remained blocked at this stage and none had progressed to the DN3 stage. To rule out the possibility that the cells were not following the normal T-cell differentiation pathway, TLX1/EML1-ABL1-ICN1 cells were examined for CD4 and CD8 expression at the end of the co-culture; the cells were negative as expected (data not shown). These findings are similar to the DN2 block of T cell differentiation we previously observed for TLX1-expressing primary murine fetal liver cells in fetal thymic organ cultures [34] and others previously reported in Lck-TLX1-transgenic mice [10,12].

Cells were sorted from the indicated stages (DN1, DN2 and DN3) and qRT-PCR was performed to assess the expression of Bcl11b, Cd3e and Lmo2 mRNAs [32]. Bcl11b and Cd3e expression were upregulated at the DN3 stage of the differentiating primary bone marrow progenitor cells as expected (Figure 1). TLX1-immortalized cells, similar to multipotential bone marrow progenitors [32], express Lmo2 as determined previously by Northern blot analysis [28]; and this result was confirmed by qRT-PCR for the TLX1/EML1-ABL1-ICN1 cells (Figure 1). Downregulation of Lmo2 expression in the DN2 subset of the TLX1/EML1-ABL1-ICN1 cells further supports the view that these TLX1-expressing cells have the potential to begin differentiating down the T-cell lineage [32]. Moreover, their inability to upregulate Bcl11b and Cd3e expression is consistent with the failure of the cells to transit

Figure 2: TLX1-expressing DN2mt cells progress toward aneuploidy after treatment with paclitaxel. (A) Flow cytometry was performed to analyze the cell cycle of TLX1-expressing DN2mt (TLX1-positive) or TLX1-negative progenitor cells treated with vehicle control, 0.1 µM or 0.01 µM paclitaxel as indicated. Cells were fixed with 70% ethanol and stained with PI/RNase A solution. Flow cytometry data were acquired using CellQuest software on a FACScan instrument and analysis was performed using ModFit LT software. Red peaks indicate diploid cell cycle and yellow peaks indicate aneuploid cell cycle. Data are representative of two independent experiments. (B) Heat map representation of cell cycle-regulated genes that are TLX1 binding targets [12] in TLX1-expressing DN2mt (TLX1-positive) versus TLX1-negative progenitor cells after hierarchical clustering. TLX1(T247I), bone marrow progenitor cells immortalized with a mutant TLX1 protein containing an isoleucine instead of threonine at position 247 (position 47 within the homeodomain) [21]; TLX1+ T-ALL, murine TLX1+ CD4+CD8+ T-ALL-like cells [11]. (C) Heat map representation of the expression levels of CIN-survival genes [79] that are TLX1 binding targets [12] in TLX1-expressing DN2mt (TLX1-positive) versus TLX1-negative progenitor cells after hierarchical clustering.

the DN2mt (DN2 myeloid-T)-DN2t (DN2 T-lineage determined) T-lineage commitment step [32].

TLX1-expressing DN2mt cells progress toward aneuploidy

Aneuploidy is one of the most common abnormalities of cancer cells [66]. It was reported previously that TLX1 regulates the expression of genes involved in mitosis [12,14-16] and this mechanism may contribute to aneuploidy and early stages of transformation in the context of T-ALL development [12]. In an earlier study, we demonstrated that aneuploidy was not necessary for immortalization by TLX1 [28]. In that study, we performed cytogenetic analyses of 7 cell lines. All except one of cell lines had a diploid 40, XX karyotype by G-banding of chromosome spreads, consistent with their derivation from normal bone marrow cells of female mice. The exception exhibited a 40,X0,+16 [15] karyotype (two cells were 40, XX and three cells had a hypodiploid karyotype), with loss of one copy of the X chromosome and trisomy 16 confirmed by fluorescence in-situ hybridization. Similarly, Hough et al. [15] reported that enforced TLX1 expression in primary B cells did not cause missegregation of chromosomes but conferred an increased susceptibility to segregation errors following treatment with microtubule inhibitors [14]. Therefore, we were interested in determining whether constitutive TLX1 expression in immortalized DN2mt cells conferred an increased susceptibility to aneuploidy following treatment with microtubule-targeting drugs. To further dissect out the role of TLX1 in the regulation of cell cycle- and mitosis-related genes in transformation, we assessed mitotic checkpoint integrity by cell cycle analysis. The TLX1-expressing DN2mt cell line used for these experiments was previously shown to have a diploid karyotype [28]. TLX1-negative control cells were an IL-3-dependent hematopoietic progenitor line which, similar to TLX1-immortalized cells, can be induced to generate CD11b/Mac-1$^+$ Ly-6G/Gr-1$^+$ myeloid cells [36]. The cells were synchronized by removing IL-3 for 24 hours prior to treatment with the microtubule poison paclitaxel [67], followed by re-addition of IL-3 during treatment [51]. When treated with 0.1 μM paclitaxel for 24 hours, TLX1-expressing DN2mt cells bypassed the mitotic checkpoint and progressed toward polyploidy whereas the TLX1-negative control cells were arrested in G_2M (Figure 2A). Notably, TLX1-expressing DN2mt cells were highly sensitive to the mitotic inhibitor, with significant tetraploidy observed at 10-fold lower levels of the drug (0.01 μM paclitaxel for 48 hours) in the absence of a corresponding effect on the control progenitor cells (Figure 2A).

TLX1-expressing DN2mt cells express elevated levels of target genes involved in DNA replication and mitosis

Cells develop aneuploidy by errors in cell division or from DNA breaks, thereby resulting in changes in chromosome number or gene rearrangement. Cell cycle checkpoints provide a barrier to genetic instability and tumors exhibiting CIN frequently overexpress cell cycle checkpoint control genes [68]. Studies of the SV40 large T and HPV16 E6 oncoproteins provide precedent for dysregulation of mitotic checkpoints and transformation [69-71]. For example, cells expressing SV40 large T antigen have increased expression of the mitotic regulatory proteins cyclin A, cyclin B and Cdc25C [71].

Enforced expression of TLX1 in a human TLX1-negative T-ALL cell line (TAL1$^+$ Jurkat cells) previously led to aberrant bypass of G_2/M arrest induced by ionizing radiation [72]. Moreover, Hough et al. [15] reported that TLX1 conferred a heightened susceptibility to aneuploidy of primary B cells and B cell tumors in IgHμ-HOX11^{Tg} mice following aneugenic insults with microtubule targeting agents. This latter investigation identified elevated expression of the cyclin A, cyclin B1

and Cdc20 mitotic regulatory proteins as correlating with the ability of TLX1 to facilitate bypass of spindle checkpoint arrest [14]. In a follow up study, Chen et al. confirmed that Ccnb1 (encoding cyclin B1) is a direct TLX1 target, transcriptional activation of which was associated with accelerated progression through the G_2/M phase of the cell cycle [16]. In other work, Sansregret et al. reported that Cut homeobox 1 (CUX1) causes CIN by activating a transcriptional program that prevents multipolar divisions and enables the survival of tetraploid cells that evolve to become genetically unstable and tumorigenic [73]. A number of genes involved in DNA replication and bipolar mitosis that were transcriptionally upregulated by CUX1 are TLX1 ChIP-chip binding targets in T-ALL [12,73]. Interestingly, similar to TLX1 [24], CUX1 also regulates G_1/S progression [74] and many of the genes activated by CUX1 were identified as TLX1 binding targets [12].

We first compiled a set of TLX1 ChIP-chip target genes [12] involved in the G_2/M as well as the G_1/S transcriptional programs that were previously found to be upregulated at the mRNA or protein levels upon ectopic TLX1 expression in various experimental systems. These included Ccna2, Ccnb1, Ccnb2, Cdc20 [14,16], Cdc25a [26], Cdc6, Mcm2, Mcm4, Mcm5, Mcm6, Rad51, Top2a and Ttk [24]. To this set, we added TLX1 ChIP-chip targets that were shown to be directly activated by CUX1 and relevant to the establishment of bipolar mitoses leading to CIN (Aurkb, Bub1, Bub3, Camk2d, Cenpa, Cenpe, Kifc1, Kif2c, Mad2l1, Nek2, Ttk and Zw10) [73]. We merged this list with TLX1 ChiP-chip targets that regulate the G_1/S transition that were shown to be directly activated by CUX1 (Ccna2, Cdc25b, Cdc7, Cdc25c, Cdc45l, Mcm7, Rad51 and Pola2) [74].

We performed a microarray gene expression analysis of TLX1-expressing DN2mt cells versus the TLX1-negative control progenitor cells studied in Figure 2A and initially focused our analysis on the above genes. We also examined their expression levels in a murine TLX1-induced T-ALL [11] and in an IL-3-dependent murine hematopoietic progenitor cell line established by expression of a mutant TLX1 protein containing an isoleucine instead of threonine at position 247 (position 47 within the homeodomain) [21] (referred to herein as TLX1 Thr247Ile). This substitution restricts in vitro DNA binding of TLX1 from a TAANTG to a TAATTG core motif [75-77]. Among other genes, this gene profiling analysis revealed elevated expression of Ccna2 (cyclin A2), Ccnb1 (cyclin B1) and Ccnb2 (cyclin B2) in TLX1-expressing DN2mt versus TLX1-negative progenitor cells, similar to the results obtained by Hough et al. for primary TLX1-expressing B cells that exhibited a heightened susceptibility to aneuploidy following treatment with microtubule targeting agents [15]. All three genes were highly expressed in murine TLX1$^+$ T-ALL cells and high level expression correlated with the presence of Thr247 in the wild-type TLX1 protein (Figure 2B). These results are consistent with the findings of Chen et al. who showed that Thr247-dependent upregulation of CCNB1 by ectopic TLX1 expression was associated with dysfunction of the spindle assembly checkpoint in fibroblast and T-ALL cell line models [16]. Finally, the data are concordant with the observation that high levels of CCNA2 expression specifically associate with the TLX1$^+$ subtype in T-ALL patient samples [1].

CIN-survival genes are variably expressed in TLX1-expressing DN2mt cells

In addition to stimulating CIN, paclitaxel treatment of TLX1-expressing DN2mt cells also induced a high frequency of cell death, as evidenced by a striking increase in the fraction of cells with subG$_1$ DNA content (Figure 2A). Although CIN leading to aneuploidy is

associated with poor prognosis in human solid tumors [68], a greater percentage of TLX1+ T-ALLs are aneuploid (40-50%) compared to non-TLX1 subtypes (~11%) yet reportedly exhibit a more favorable outcome [78]. Swanton et al. identified a set of 50 genes repressed in sensitive cell lines treated with microtubule-stabilizing agents such as paclitaxel [79], and observed that these genes are overexpressed in different human solid tumors exhibiting CIN [68]. Silencing 22 out of 50 of these genes, many of which are involved in DNA repair, caused tumor cell death, suggesting that these genes are involved in the survival of aneuploid cells [79]. We noted that 41 out of 50 of these CIN-survival genes are TLX1 ChiP-chip targets [12] and, with some exceptions (i.e., Bub3, Cdc6, Mcm6 and Top2a), did not overlap with the list of TLX1 transcriptional targets involved in DNA replication and mitosis (Figure 2B). As shown in Figure 2C and consistent with the exquisite sensitivity of TLX1-expressing DN2mt cells to paclitaxel, comparative gene profiling analysis revealed that instead of being overexpressed, the relative expression levels of many CIN-survival-related TLX1 target genes were reduced in TLX1-expressing DN2mt cells versus TLX1-negative control cells.

Enforced BCL11B expression in human TLX1+ T-ALL cells confers resistance to the topoisomerase IIα poison etoposide

Of those TLX1 direct target genes more highly expressed in TLX1-expressing DN2mt cells and which display TLX1 Thr247-dependent upregulation, Top2a, encoding topoisomerase IIα, is of particular interest (Figure 2B and 2C). Topoisomerase IIα is essential for DNA replication, transcription and chromosome segregation, and is a clinically important molecular target for cancer chemotherapy [80]. High levels of topoisomerase IIα correlate with sensitivity of certain cancers to intercalating agents (e.g., doxorubicin) and epipodophyllotoxins such as etoposide [81]. It is noteworthy that high levels of TOP2A expression distinguish TLX1+ T-ALL cases from other T-ALL subtypes [1]. Consistent with the observations involving TLX1+ T-ALL patient samples, we previously found that TLX1+ ALL-SIL cells express high levels of TOP2A and that ectopic expression of TLX1 in TLX1-negative Jurkat T-ALL cells resulted in TOP2A upregulation [24].

TLX1+ T-ALL cells characteristically have a CD4+CD8+ Double Positive (DP) phenotype, resembling an early cortical thymocyte [1-3]; and we have provided evidence that aberrant TLX1 expression plays a role in the differentiation arrest by performing shRNA-

Figure 3: Enforced BCL11B expression in human TLX1+ T-ALL cells confers resistance to the topoisomerase IIα poison etoposide. ALL-SIL cells mock transduced or ectopically expressing BCL11B (BCL11B) were treated with etoposide at the indicated concentrations for 3 hours. Cell viability was measured using the alamarBlue reagent. Results are the average of 3 technical replicates ± SD. P values indicate significant differences in cell counts. Data are representative of two independent experiments.

mediated knockdown of TLX1 transcripts in ALL-SIL cells [53,54]. DP thymocytes normally express BCL11B, and Avram showed that BCL11B-deficient DP thymocytes are more prone to spontaneous cell death [82]. Studies in other systems have indicated that upregulation of BCL11B expression increases resistance to genotoxic stress in some circumstances [83,84]. As noted above, De Keersmaecker et al. reported that BCL11B was repressed by TLX1 in ALL-SIL, becoming transcriptionally upregulated after TLX1 knockdown [12]. However, we previously demonstrated that TLX1 knockdown in ALL-SIL was associated with significant cell death [53,54]. Therefore, to investigate the potential role of BCL11B in providing protection from DNA damage-induced apoptosis in T-ALL, we overexpressed exogenous BCL11B in ALL-SIL cells using the MSCV-BCL11B retroviral vector [40]. BCL11B-expressing and mock transduced ALL-SIL cells were treated with different concentrations of etoposide and cell viability was measured using the alamar Blue reagent as previously described [52]. As seen in Figure 3, enforced BCL11B expression in ALL-SIL cells provided significant protection against etoposide-induced cell death at all concentrations examined.

Discussion

Accumulated data from our laboratory and others indicate that TLX1 functions to regulate transcription by either activating or repressing gene expression, thereby controlling the survival and differentiation block associated with leukemic T-ALL cells [12,13,16,21,23,24,26,27,53,54,75,85-92]. Disruption of tumor suppressor pathways is a recurring feature associated with the immortalization of cells in culture and the progression of normal somatic cells to malignancy. Of these, the p53 tumor suppressor pathway, which is inactivated in virtually all cancers [93], was first identified through studies of the SV40 large T and HPV16 E6 proteins [94]. In addition to targeting p53, these viral oncoproteins also compromise mitotic checkpoints by upregulating the expression of mitotic regulatory proteins such as cyclin A and cyclin B [69-71]. The data presented herein confirm and extend previous reports that aberrant TLX1 expression induces mitotic defects and allows strong parallels to be drawn with these DNA tumor virus oncogenes [12,14-16,24].

We think it is especially noteworthy that we found no evidence of deletions or mutations within p53, which are common events during spontaneous cellular immortalization [57] but rarely found in T-ALL [95]. We propose that ectopic TLX1 expression complements IL-3 signaling to suppress p53 levels [61]. The mechanistic details remain to be elaborated. However, a mechanism involving transcriptional repression is suggested by the fact that p53 is a TLX1 binding target [12]. Our previous structure-function analysis of TLX1 provides indirect support for this speculation [21]. In that study, we found that specific point mutations within the TLX1 homeodomain—in particular, alanine substitution of an invariant asparagine residue at position 251 that is indispensable for efficient homeodomain-DNA binding [96]—abrogated TLX1 immortalizing function. This scenario would also explain why the mutant TLX1 protein containing an isoleucine instead of threonine at position 247 retains immortalizing potential [21]. As noted earlier, the Thr247Ile substitution restricts TLX1 *in vitro* DNA binding activity from TAA(G/C/T) to the prototypical homeodomain TAAT core motif [75-77]. Transcriptional regulation of p53 via a TAAT core motif in the p53 promoter was previously demonstrated for another homeodomain protein [97].

A myeloid-based model of hematopoiesis has been described in
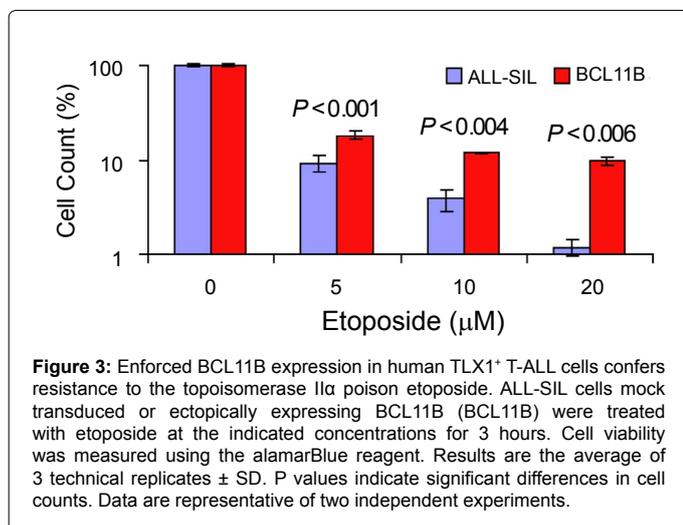
which myeloid potential is retained in an early stage of branches toward erythroid, T- and B-cell lineages [29] (reviewed in [33]). In this model, the zinc finger transcription factor Bcl11b serves as a restriction point at the DN2mt stage of T-cell differentiation, progression past which is associated with termination of myeloid, dendritic and natural killer cell developmental potential [30-32]. DN2t progenitors traversing this step are restrained to the T-cell lineage, progressing to CD4+CD8+ DP cells. We initially reported that hematopoietic stem cell-directed expression of TLX1 induced T-ALL-like tumors in mice with long latency while giving rise to immortalized progenitor cell lines at high frequency under myeloid-supportive culture conditions [11,17]. Although TLX1+ T-ALL are associated with a CD4+CD8+ DP surface phenotype, one of the murine TLX1+ T-ALL-like tumors that arose consisted of cells resembling DN1/DN2 thymocytes [11]. We unexpectedly found in other work that enforced expression of TLX1 in murine fetal liver precursors and human cord blood CD34+ stem/progenitor cells assayed in fetal thymic organ cultures disrupted T-cell differentiation prior to the DP stage, arresting the cells at the DN2 stage of thymocyte development [34]. In this paper, we reconcile these apparently discordant results by demonstrating that the TLX1-derived cell lines represent immortalized DN2mt progenitors blocked at the Bcl11b-controlled T-lineage restriction point defined within the myeloid-based hematopoiesis model.

A similar arrest of thymocytes within the DN2 compartment is observed in transgenic mice in which TLX1 was placed under the control of the Lck proximal promoter [10,12]. In fact, transgenic mice in which the expression of GFP is driven by the Lck proximal promoter were used by Kawamoto et al. to delineate the Bcl11b-dependent DN2mt-DN2t transition step [98]. They found that DN2 cells could be subdivided into GFP- and GFP+ cells: GFP- DN2 cells (which they designated DN2mt) retained the potential to produce macrophages, dendritic cells and natural killer cells while Lck promoter-driven GFP+ DN2 cells (which they designated DN2t) failed to produce these non-T-cell lineages. Consistent with all of these observations and the inability of TLX1-expressing DN2mt cells to upregulate Bcl11b, De Keersmaecker et al. reported that BCL11B is a direct transcriptional target downregulated by TLX1 in the human T-ALL cell line ALL-SIL [12]. These researchers also identified recurrent deletions and mutations of the Bcl11b gene in the T-ALL-like tumors that developed in Lck-TLX1 transgenic mice and involving human BCL11B in TLX1+ patient leukemia samples, suggesting that it acts as a tumor suppressor gene in TLX1+ T-ALL [12].

The above notwithstanding, ALL-SIL cells, like the majority of TLX1+ T-ALL cases [1-3], express a predominantly CD4+CD8+ DP phenotype [53,54]. In this regard, it is important to note that genetic analyses in the mouse have indicated that Bcl11b also plays a critical role in the maturation of CD4+CD8+ DP thymocytes into CD4+ and CD8+ single-positive T cells [82]. We previously demonstrated that shRNA-mediated knockdown of TLX1 transcripts in ALL-SIL cells released the DP differentiation block [53,54]. However, Bcl11b-deficient DP thymocytes rearrange the T cell receptor (TCR) α locus whereas TLX1+ T-ALL cells are arrested at an earlier cortical DP stage prior to TCRα chain expression [1-3]. Normally, transcriptional access to the TCRα locus, which is under the control of the Eα enhancer, occurs at the late DN to CD4+CD8+ DP transition. Eα-mediated transcriptional activity depends on the cooperative binding of the ETS1, RUNX1 and LEF1 transcription factors. Dadi et al. recently found that TLX1 interacts with ETS1 to repress Eα activity, thereby preventing TCR-Jα rearrangement and further differentiation [92]. It is noteworthy that both RUNX1 and

LEF1 are converted to transcriptional repressors by interaction with the Groucho/transducin-like Enhancer of split (Gro/TLE) family of corepressors and this interaction inhibits activation of the Eα enhancer [99]. Silencing of the Eα enhancer in TLX1+ T-ALL cells was associated with increased concentration of H3K27me3, a marker of repressive chromatin, across the TCRα locus [92]. Along these lines, we found that TLX1 interacts with Gro/TLE corepressors [91] and that shRNA-mediated knockdown of TLE transcripts in ALL-SIL cells also released the DP differentiation block [54]. As Gro/TLE corepressors facilitate transcriptional silencing via a mechanism that involves in H3K27 methylation [100], it is tempting to speculate that TLX1 recruitment of Gro/TLE family members to the Eα enhancer also contributes to the early cortical DP differentiation block in TLX1+ T-ALL cases.

In agreement with results obtained by Hough et al. for primary B cells inappropriately expressing TLX1 [14,15], we found that diploid TLX1-expressing DN2mt cells exhibited aberrant bypass of spindle checkpoint arrest, displayed chromosomal instability and progressed toward aneuploidy upon treatment with a mitotic inhibitor. Furthermore, in accord with the findings of these investigators [16], we observed Thr247-dependent TLX1-mediated upregulation of Ccnb1 as well as other mitotic regulators (e.g., Ccna2, Ccnb2) implicated in CIN in other systems [68-71,73]. The data are strengthened by the observation of Ferrando et al. that high levels of CCNA2 expression specifically associate with the TLX1+ subtype of T-ALL [1]. Collectively, the data support a mechanism posited by De Keersmaecker et al. in which TLX1-promoted aneuploid cells progressively evolve toward malignancy [12]. Notably, a similar mechanism in the context of mammary tumorigenesis was validated for the CUX1 homeodomain oncoprotein, which shares significant overlap of binding targets with TLX1 [12,73]. However, in contrast to the CUX1 findings, as well as our results herein, those of Hough et al. and landmark studies of SV40 large T and HPV16 E6 oncoproteins, De Keersmaecker et al. proposed that downregulation of other mitotic regulatory genes was responsible for abnormal TLX1 mitotic checkpoint control [12]. Upon careful examination of their mitotic cell cycle gene set, we detected only a subtle change in the expression of Chek1 in premalignant TLX1-expressing DN2mt cells and no consistent downregulation of the other genes that they proposed as being integral to the process (Figure 2C; Figure S4). We surmise that a reason for the discrepancy might be related to a flaw in their experimental design. De Keersmaecker et al. based on their conclusions on gene expression profiling analyses of DN2 cells obtained from preleukemic Lck-TLX1 transgenic and normal mice. Whereas the sorted transgenic Lck-TLX1 DN2 cells would consist of DN2mt-arrested cells undergoing apoptosis, the sorted control DN2 cells would be composed of a mixture of DN2mt and more differentiated Bcl11b-expressing DN2t populations [98].

Our findings that TLX1-expressing DN2mt cells are exquisitely sensitive to paclitaxel-induced death may relate to observations that aneuploid TLX1+ T-ALLs reportedly exhibit a favorable treatment outcome [78]. T-ALL treatment regimens typically contain microtubule-targeting drugs [101]. Our gene expression analysis of TLX1-expressing DN2mt cells accurately identified upregulated expression of Top2a encoding topoisomerase IIα, high levels of which distinguish TLX1+ T-ALL cases from other T-ALL subtypes [1]. Moreover, ectopic expression of BCL11B in the TLX1+ ALL-SIL T-ALL cell line conferred resistance to the topoisomerase IIα poison etoposide. In accord with other investigations [84,102], we found that BCL11B expression was associated with a reduced proliferation rate (unpublished data). Of relevance to our findings, Schmidt and colleagues reported that BCL11B overexpression in TLX1-negative T-ALL cell lines conferred resistance

to etoposide-induced death through a mechanism associated with cell cycle delay at the G_1/S phase [84]. In view of our earlier findings that TLX1 also stimulates G_1/S progression [24], it will be interesting to determine whether a similar mechanism operates in TLX1$^+$ T-ALL cells.

Conclusion

Taken together with previous findings, the data support a mechanism of TLX1 leukemogenic activity linked to chromosomal instability resulting from upregulated expression of target genes involved in DNA replication and mitosis, including Top2a, Ccna2, Ccnb1 and Ccnb2. Moreover, since most T-ALL combination chemotherapies include a topoisomerase IIα inhibitor [101], repression of BCL11B expression may provide part of the explanation for the observation that aneuploid DNA content in TLX1$^+$ T-ALL does not necessarily portend an unfavorable prognosis. The TLX1-expressing DN2mt cell culture model should help further our understanding of the mechanisms of TLX1-mediated evolution to malignancy and has the potential to be a useful predictor of disease response to novel therapeutic agents in TLX1$^+$ T-ALL. For example, Idi1 (encoding isopentenyl diphosphate isomerase 1) and Fdft1 (encoding squalene synthase), both of which are involved in cholesterol biosynthesis, displayed Thr247-dependent upregulation by TLX1 in the DN2mt gene expression profiling experiments (Figure 2C). Successful follow up of these observations might suggest incorporation of cholesterol-modulating agents into future TLX1$^+$ T-ALL chemotherapeutic regimens [103-106].

References

1. Ferrando AA, Neuberg DS, Staunton J, Loh ML, Huard C, et al. (2002) Gene expression signatures define novel oncogenic pathways in T cell acute lymphoblastic leukemia. Cancer Cell 1: 75-87.

2. Asnafi V, Beldjord K, Libura M, Villarese P, Millien C, et al. (2004) Age-related phenotypic and oncogenic differences in T-cell acute lymphoblastic leukemias may reflect thymic atrophy. Blood 104: 4173-4180.

3. Soulier J, Clappier E, Cayuela JM, Regnault A, Garcia-Peydro M, et al. (2005) HOXA genes are included in genetic and biologic networks defining human acute T-cell leukemia (T-ALL). Blood 106: 274-286.

4. Owens BM, Hawley RG (2002) HOX and non-HOX homeobox genes in leukemic hematopoiesis. Stem Cells 20: 364-379.

5. Aifantis I, Raetz E, Buonamici S (2008) Molecular pathogenesis of T-cell leukaemia and lymphoma. Nat Rev Immunol 8: 380-390.

6. Hatano M, Roberts CW, Minden M, Crist WM, Korsmeyer SJ (1991) Deregulation of a homeobox gene, HOX11, by the t(10;14) in T cell leukemia. Science 253: 79-82.

7. Kennedy MA, Gonzalez-Sarmiento R, Kees UR, Lampert F, Dear N, et al. (1991) HOX11, a homeobox-containing T-cell oncogene on human chromosome 10q24. Proc Natl Acad Sci USA 88: 8900-8904.

8. Lu M, Gong ZY, Shen WF, Ho AD (1991) The tcl-3 proto-oncogene altered by chromosomal translocation in T-cell leukemia codes for a homeobox protein. EMBO J 10: 2905-2910.

9. Dube ID, Kamel-Reid S, Yuan CC, Lu M, Wu X, et al. (1991) A novel human homeobox gene lies at the chromosome 10 breakpoint in lymphoid neoplasias with chromosomal translocation t(10;14). Blood 78: 2996-3003.

10. Hatano M, Roberts CW, Kawabe T, Shutter J, Korsmeyer SJ (1992) Cell cycle progression, cell death and T cell lymphoma in HOX11 transgenic mice. Blood 80: 355a.

11. Hawley RG, Fong AZ, Reis MD, Zhang N, Lu M, et al. (1997) Transforming function of the HOX11/TCL3 homeobox gene. Cancer Res 57: 337-345.

12. De Keersmaecker K, Real PJ, Gatta GD, Palomero T, Sulis ML, et al. (2010) The TLX1 oncogene drives aneuploidy in T cell transformation. Nat Med 16: 1321-1327.

13. Rakowski LA, Lehotzky EA, Chiang MY (2011) Transient responses to NOTCH and TLX1/HOX11 inhibition in T-cell acute lymphoblastic leukemia/lymphoma. PLoS One 6: e16761.

14. Chen E, Lim MS, Rosic-Kablar S, Liu J, Jolicoeur P, et al. (2006) Dysregulated expression of mitotic regulators is associated with B-cell lymphomagenesis in HOX11-transgenic mice. Oncogene 25: 2575-2587.

15. Chen E, Kwon YT, Lim MS, Dube ID, Hough MR (2006) Loss of Ubr1 promotes aneuploidy and accelerates B-cell lymphomagenesis in TLX1/HOX11-transgenic mice. Oncogene 25: 5752-5763.

16. Chen E, Huang X, Zheng Y, Li YJ, Chesney A, et al. (2010) Phosphorylation of HOX11/TLX1 on Threonine-247 during mitosis modulates expression of cyclin B1. Mol Cancer 9: 246.

17. Hawley RG, Fong AZ, Lu M, Hawley TS (1994) The HOX11 homeobox-containing gene of human leukemia immortalizes murine hematopoietic precursors. Oncogene 9: 1-12.

18. Yu WM, Hawley TS, Hawley RG, Qu CK (2002) Immortalization of yolk sac-derived precursor cells. Blood 100: 3828-3831.

19. Yu WM, Hawley TS, Hawley RG, Qu CK (2003) Catalytic-dependent and -independent roles of SHP-2 tyrosine phosphatase in interleukin-3 signaling. Oncogene 22: 5995-6004.

20. Keller G, Wall C, Fong AZ, Hawley TS, Hawley RG (1998) Overexpression of HOX11 leads to the immortalization of embryonic precursors with both primitive and definitive hematopoietic potential. Blood 92: 877-887.

21. Owens BM, Zhu YX, Suen TC, Wang PX, Greenblatt JF, et al. (2003) Specific homeodomain-DNA interactions are required for HOX11-mediated transformation. Blood 101: 4966-4974.

22. Hawley RG, Hawley TS, Cantor AB (2008) TLX1 (HOX11) immortalization of embryonic stem cell-derived and primary murine hematopoietic progenitors. Curr Protoc Stem Cell Biol. 7: 1F.7.1-1F.7.19.

23. Greene WK, Ford J, Dixon D, Tilbrook PA, Watt PM, et al. (2002) Enforced expression of HOX11 is associated with an immature phenotype in J2E erythroid cells. Br J Haematol 118: 909-917.

24. Riz I, Hawley RG (2005) G1/S transcriptional networks modulated by the HOX11/TLX1 oncogene of T-cell acute lymphoblastic leukemia. Oncogene 24: 5561-5575.

25. Su X, Drabkin H, Clappier E, Morgado E, Busson M, et al. (2006) Transforming potential of the T-cell acute lymphoblastic leukemia-associated homeobox genes HOXA13, TLX1, and TLX3. Genes Chromosomes Cancer 45: 846-855.

26. Dixon DN, Izon DJ, Dagger S, Callow MJ, Taplin RH, et al. (2007) TLX1/HOX11 transcription factor inhibits differentiation and promotes a non-haemopoietic phenotype in murine bone marrow cells. Br J Haematol 138: 54-67.

27. Riz I, Akimov SS, Eaker SS, Baxter KK, Lee HJ, et al. (2007) TLX1/HOX11-induced hematopoietic differentiation blockade. Oncogene 26: 4115-4123.

28. Zweier-Renn LA, Hawley TS, Burkett S, Ramezani A, Riz I, et al. (2010) Hematopoietic immortalizing function of the NKL-subclass homeobox gene TLX1. Genes Chromosomes Cancer 49: 119-131.

29. Wada H, Masuda K, Satoh R, Kakugawa K, Ikawa T, et al. (2008) Adult T-cell progenitors retain myeloid potential. Nature 452: 768-772.

30. Li P, Burke S, Wang J, Chen X, Ortiz M, et al. (2010) Reprogramming of T cells to natural killer-like cells upon Bcl11b deletion. Science 329: 85-89.

31. Li L, Leid M, Rothenberg EV (2010) An early T cell lineage commitment checkpoint dependent on the transcription factor Bcl11b. Science 329: 89-93.

32. Ikawa T, Hirose S, Masuda K, Kakugawa K, Satoh R, et al. (2010) An essential

developmental checkpoint for production of the T cell lineage. Science 329: 93-96.

33. Kawamoto H, Ikawa T, Masuda K, Wada H, Katsura Y (2010) A map for lineage restriction of progenitors during hematopoiesis: the essence of the myeloid-based model. Immunol Rev 238: 23-36.

34. Owens BM, Hawley TS, Spain LM, Kerkel KA, Hawley RG (2006) *TLX1/HOX11*-mediated disruption of primary thymocyte differentiation prior to the CD4+CD8+ double-positive stage. Br J Haematol 132: 216-229.

35. Palacios R, Kiefer M, Brockhaus M, Karjalainen K, Dembic Z, et al. (1987) Molecular, cellular, and functional properties of bone marrow T lymphocyte progenitor clones. J Exp Med 166: 12-32.

36. Hawley RG, Fong AZ, Ngan BY, de Lanux VM, Clark SC, et al. (1993) Progenitor cell hyperplasia with rare development of myeloid leukemia in interleukin 11 bone marrow chimeras. J Exp Med 178: 1175-1188.

37. Ramezani A, Hawley TS, Hawley RG (2008) Combinatorial incorporation of enhancer-blocking components of the chicken beta-globin 5'HS4 and human T-cell receptor alpha/delta BEAD-1 insulators in self-inactivating retroviral vectors reduces their genotoxic potential. Stem Cells 26: 3257-3266.

38. De Keersmaecker K, Graux C, Odero MD, Mentens N, Somers R, et al. (2005) Fusion of EML1 to ABL1 in T-cell acute lymphoblastic leukemia with cryptic t(9;14)(q34;q32). Blood 105: 4849-4852.

39. Pui JC, Allman D, Xu L, DeRocco S, Karnell FG, et al. (1999) Notch1 expression in early lymphopoiesis influences B versus T lineage determination. Immunity 11: 299-308.

40. Cismasiu VB, Ghanta S, Duque J, Albu DI, Chen HM, et al. (2006) BCL11B participates in the activation of IL2 gene expression in CD4+ T lymphocytes. Blood 108: 2695-2702.

41. Hawley RG, Lieu FH, Fong AZ, Hawley TS (1994) Versatile retroviral vectors for potential use in gene therapy. Gene Ther 1: 136-138.

42. Modlich U, Bohne J, Schmidt M, von Kalle C, Knoss S, et al. (2006) Cell-culture assays reveal the importance of retroviral vector design for insertional genotoxicity. Blood 108: 2545-2553.

43. Hawley RG, Hawley TS, Fong AZ, Quinto C, Collins M, et al. (1996) Thrombopoietic potential and serial repopulating ability of murine hematopoietic stem cells constitutively expressing interleukin 11. Proc Natl Acad Sci USA 93: 10297-10302.

44. Akagi K, Suzuki T, Stephens RM, Jenkins NA, Copeland NG (2004) RTCGD: retroviral tagged cancer gene database. Nucleic Acids Res 32: D523-D527.

45. Kustikova OS, Geiger H, Li Z, Brugman MH, Chambers SM, et al. (2007) Retroviral vector insertion sites associated with dominant hematopoietic clones mark "stemness" pathways. Blood 109: 1897-1907.

46. Haviernik P, Schmidt M, Hu X, Wolff L (2003) Consistent inactivation of p19(Arf) but not p15(Ink4b) in murine myeloid cells transformed in vivo by deregulated c-Myc. Oncogene 22: 1600-1610.

47. Yin B, Kogan SC, Dickins RA, Lowe SW, Largaespada DA (2006) Trp53 loss during in vitro selection contributes to acquired Ara-C resistance in acute myeloid leukemia. Exp Hematol 34: 631-641.

48. Schmitt TM, Ciofani M, Petrie HT, Zuniga-Pflucker JC (2004) Maintenance of T cell specification and differentiation requires recurrent notch receptor-ligand interactions. J Exp Med 200: 469-479.

49. Wang H, Pierce LJ, Spangrude GJ (2006) Distinct roles of IL-7 and stem cell factor in the OP9-DL1 T-cell differentiation culture system. Exp Hematol 34: 1730-1740.

50. Schmitt TM, de Pooter RF, Gronski MA, Cho SK, Ohashi PS, et al. (2004) Induction of T cell development and establishment of T cell competence from embryonic stem cells differentiated in vitro. Nat Immunol 5: 410-417.

51. Abrams SL, Steelman LS, Shelton JG, Chappell W, Basecke J, et al. (2010) Enhancing therapeutic efficacy by targeting non-oncogene addicted cells with combinations of signal transduction inhibitors and chemotherapy. Cell Cycle 9: 1839-1846.

52. Riz I, Zweier-Renn LA, Toma I, Hawley TS, Hawley RG (2011) Apoptotic role of IKK in T-ALL therapeutic response. Mol Cancer Res 9: 979-984.

53. Riz I, Hawley TS, Johnston H, Hawley RG (2009) Role of *TLX1* in T-cell acute lymphoblastic leukaemia pathogenesis. Br J Haematol 145: 140-143.

54. Riz I, Hawley TS, Luu TV, Lee NH, Hawley RG (2010) TLX1 and NOTCH coregulate transcription in T cell acute lymphoblastic leukemia cells. Mol Cancer 9: 181.

55. Du Y, Jenkins NA, Copeland NG (2005) Insertional mutagenesis identifies genes that promote the immortalization of primary bone marrow progenitor cells. Blood 106: 3932-3939.

56. Krug U, Ganser A, Koeffler HP (2002) Tumor suppressor genes in normal and malignant hematopoiesis. Oncogene 21: 3475-3495.

57. Harvey DM, Levine AJ (1991) p53 alteration is a common event in the spontaneous immortalization of primary BALB/c murine embryo fibroblasts. Genes Dev 5: 2375-2385.

58. Kamijo T, Zindy F, Roussel MF, Quelle DE, Downing JR, et al. (1997) Tumor suppression at the mouse INK4a locus mediated by the alternative reading frame product p19ARF. Cell 91: 649-659.

59. Zindy F, Eischen CM, Randle DH, Kamijo T, Cleveland JL, et al. (1998) Myc signaling via the ARF tumor suppressor regulates p53-dependent apoptosis and immortalization. Genes Dev 12: 2424-2433.

60. Schmidt M, Koller R, Haviernik P, Bies J, Maciag K, et al. (2001) Deregulated c-Myb expression in murine myeloid leukemias prevents the up-regulation of p15(INK4b) normally associated with differentiation. Oncogene 20: 6205-6214.

61. Jabbour AM, Daunt CP, Green BD, Vogel S, Gordon L, et al. (2010) Myeloid progenitor cells lacking p53 exhibit delayed up-regulation of Puma and prolonged survival after cytokine deprivation. Blood 115: 344-352.

62. Graux C, Cools J, Melotte C, Quentmeier H, Ferrando A, et al. (2004) Fusion of NUP214 to ABL1 on amplified episomes in T-cell acute lymphoblastic leukemia. Nat Genet 36: 1084-1089.

63. De Keersmaecker K, Verachtert H, Landuyt W, De Wolf-Peeters C, Vandenberghe P, et al. (2007) EML1-ABL1 is activated by coiled coil mediated oligomerization and induces T-cell acute lymphoblastic or chronic myeloid leukemia in a mouse bone marrow transplant model. Haematologica 92: 326.

64. Weng AP, Ferrando AA, Lee W, Morris JP 4th, Silverman LB, et al. (2004) Activating mutations of NOTCH1 in human T cell acute lymphoblastic leukemia. Science 306: 269-271.

65. de Pooter R, Zuniga-Pflucker JC (2007) T-cell potential and development in vitro: the OP9-DL1 approach. Curr Opin Immunol 19: 163-168.

66. Ganem NJ, Storchova Z, Pellman D (2007) Tetraploidy, aneuploidy and cancer. Curr Opin Genet Dev 17: 157-162.

67. Jordan MA, Wilson L (2004) Microtubules as a target for anticancer drugs. Nat Rev Cancer 4: 253-265.

68. Carter SL, Eklund AC, Kohane IS, Harris LN, Szallasi Z (2006) A signature of chromosomal instability inferred from gene expression profiles predicts clinical outcome in multiple human cancers. Nat Genet 38: 1043-1048.

69. Steinmann KE, Pei XF, Stoppler H, Schlegel R, Schlegel R (1994) Elevated expression and activity of mitotic regulatory proteins in human papillomavirus-immortalized keratinocytes. Oncogene 9: 387-394.

70. Thompson DA, Belinsky G, Chang TH, Jones DL, Schlegel R, et al. (1997) The human papillomavirus-16 E6 oncoprotein decreases the vigilance of mitotic checkpoints. Oncogene 15: 3025-3035.

71. Chang TH, Ray FA, Thompson DA, Schlegel R (1997) Disregulation of mitotic checkpoints and regulatory proteins following acute expression of SV40 large T antigen in diploid human cells. Oncogene 14: 2383-2393.

72. Kawabe T, Muslin AJ, Korsmeyer SJ (1997) HOX11 interacts with protein phosphatases PP2A and PP1 and disrupts a G_2/M cell-cycle checkpoint. Nature 385: 454-458.

73. Sansregret L, Vadnais C, Livingstone J, Kwiatkowski N, Awan A, et al. (2011) Cut homeobox 1 causes chromosomal instability by promoting bipolar division after cytokinesis failure. Proc Natl Acad Sci USA 108: 1949-1954.

74. Harada R, Vadnais C, Sansregret L, Leduy L, Berube G, et al. (2008) Genome-wide location analysis and expression studies reveal a role for p110 CUX1 in the activation of DNA replication genes. Nucleic Acids Res 36: 189-202.

75. Dear TN, Sanchez-Garcia I, Rabbitts TH (1993) The HOX11 gene encodes a DNA-binding nuclear transcription factor belonging to a distinct family of homeobox genes. Proc Natl Acad Sci USA 90: 4431-4435.

76. Tang S, Breitman ML (1995) The optimal binding sequence of the Hox11 protein contains a predicted recognition core motif. Nucleic Acids Res 23: 1928-1935.

77. Shimizu H, Kang M, Iitsuka Y, Ichinose M, Tokuhisa T, et al. (2000) Identification of an optimal Ncx binding sequence required for transcriptional activation. FEBS Lett 475: 170-174.

78. Hoang T, Hoang T (2010) The T-ALL paradox in cancer. Nat Med 16: 1185-1186.

79. Swanton C, Nicke B, Schuett M, Eklund AC, Ng C, et al. (2009) Chromosomal instability determines taxane response. Proc Natl Acad Sci USA 106: 8671-8676.

80. Nitiss JL (2009) Targeting DNA topoisomerase II in cancer chemotherapy. Nat Rev Cancer 9: 338-350.

81. Davies SM, Robson CN, Davies SL, Hickson ID (1988) Nuclear topoisomerase II levels correlate with the sensitivity of mammalian cells to intercalating agents and epipodophyllotoxins. J Biol Chem 263: 17724-17729.

82. Albu DI, Feng D, Bhattacharya D, Jenkins NA, Copeland NG, et al. (2007) BCL11B is required for positive selection and survival of double-positive thymocytes. J Exp Med 204: 3003-3015.

83. Kamimura K, Mishima Y, Obata M, Endo T, Aoyagi Y, et al. (2007) Lack of Bcl11b tumor suppressor results in vulnerability to DNA replication stress and damages. Oncogene 26: 5840-5850.

84. Grabarczyk P, Nahse V, Delin M, Przybylski G, Depke M, et al. (2010) Increased expression of *Bcl11b* leads to chemoresistance accompanied by G1 accumulation. PLoS One 5: e12532.

85. Greene WK, Bahn S, Masson N, Rabbitts TH (1998) The T-cell oncogenic protein HOX11 activates *Aldh1* expression in NIH 3T3 cells but represses its expression in mouse spleen development. Mol Cell Biol 18: 7030-7037.

86. Zhang N, Shen W, Hawley RG, Lu M (1999) HOX11 interacts with CTF1 and mediates hematopoietic precursor cell immortalization. Oncogene 18: 2273-2279.

87. Allen TD, Zhu YX, Hawley TS, Hawley RG (2000) TALE homeoproteins as HOX11-interacting partners in T-cell leukemia. Leuk Lymphoma 39: 241-256.

88. Hoffmann K, Dixon DN, Greene WK, Ford J, Taplin R, et al. (2004) A microarray model system identifies potential new target genes of the proto-oncogene HOX11. Genes Chromosomes Cancer 41: 309-320.

89. Rice KL, Kees UR, Greene WK (2008) Transcriptional regulation of *FHL1* by TLX1/HOX11 is dosage, cell-type and promoter context-dependent. Biochem Biophys Res Commun 367: 707-713.

90. Rice KL, Izon DJ, Ford J, Boodhoo A, Kees UR, et al. (2008) Overexpression of stem cell associated ALDH1A1, a target of the leukemogenic transcription factor TLX1/HOX11, inhibits lymphopoiesis and promotes myelopoiesis in murine hematopoietic progenitors. Leuk Res 32: 873-883.

91. Riz I, Lee HJ, Baxter KK, Behnam R, Hawley TS, et al. (2009) Transcriptional activation by TLX1/HOX11 involves Gro/TLE corepressors. Biochem Biophys Res Commun 380: 361-365.

92. Dadi S, Le Noir S, Payet-Bornet D, Lhermitte L, Zacarias-Cabeza J, et al. (2012) TLX homeodomain oncogenes mediate T cell maturation arrest in T-ALL via interaction with ETS1 and suppression of TCRα gene expression. Cancer Cell 21: 563-576.

93. Junttila MR, Evan GI (2009) p53--a Jack of all trades but master of none. Nat Rev Cancer 9: 821-829.

94. Levine AJ, Oren M (2009) The first 30 years of p53: growing ever more complex. Nat Rev Cancer 9: 749-758.

95. Riz I, Yang W, Peng W (2011) p53 as a therapeutic target in T-ALL. In: Novel Aspects in Acute Lymphoblastic Leukemia, InTech, Rijeka: 235-258.

96. Ades SE, Sauer RT (1995) Specificity of minor-groove and major-groove interactions in a homeodomain-DNA complex. Biochemistry 34: 14601-14608.

97. Raman V, Martensen SA, Reisman D, Evron E, Odenwald WF, et al. (2000) Compromised HOXA5 function can limit p53 expression in human breast tumours. Nature 405: 974-978.

98. Masuda K, Kakugawa K, Nakayama T, Minato N, Katsura Y, et al. (2007) T cell lineage determination precedes the initiation of TCR beta gene rearrangement. J Immunol 179: 3699-3706.

99. Levanon D, Goldstein RE, Bernstein Y, Tang H, Goldenberg D, et al. (1998) Transcriptional repression by AML1 and LEF-1 is mediated by the TLE/Groucho corepressors. Proc Natl Acad Sci USA 95: 11590-11595.

100. Patel SR, Bhumbra SS, Paknikar RS, Dressler GR (2012) Epigenetic mechanisms of Groucho/Grg/TLE mediated transcriptional repression. Mol Cell 45: 185-195.

101. Pui CH, Robison LL, Look AT (2008) Acute lymphoblastic leukaemia. Lancet 371: 1030-1043.

102. Karlsson A, Nordigarden A, Jonsson JI, Soderkvist P (2007) *Bcl11b* mutations identified in murine lymphomas increase the proliferation rate of hematopoietic progenitor cells. BMC Cancer 7: 195.

103. Li HY, Appelbaum FR, Willman CL, Zager RA, Banker DE (2003) Cholesterol-modulating agents kill acute myeloid leukemia cells and sensitize them to therapeutics by blocking adaptive cholesterol responses. Blood 101: 3628-3634.

104. Bani MR, Nicoletti MI, Alkharouf NW, Ghilardi C, Petersen D, et al. (2004) Gene expression correlating with response to paclitaxel in ovarian carcinoma xenografts. Mol Cancer Ther 3: 111-121.

105. Brusselmans K, Timmermans L, Van de Sande T, Van Veldhoven PP, Guan G, et al. (2007) Squalene synthase, a determinant of Raft-associated cholesterol and modulator of cancer cell proliferation. J Biol Chem 282: 18777-18785.

106. Zhang F, Dai X, Wang Y (2012) 5-Aza-2'-deoxycytidine induced growth inhibition of leukemia cells through modulating endogenous cholesterol biosynthesis. Mol Cell Proteomics 11: M111.016915.